Weak coupling study of decoherence of a qubit in disordered magnetic environments

E. A. Winograd,[1] M.J. Rozenberg,[1, 2] and R. Chitra[3]

[1]*Departamento de Física, FCEN, Universidad de Buenos Aires,*
Ciudad Universitaria Pab.I, (1428) Buenos Aires, Argentina.
[2]*Laboratoire de Physique des Solides, CNRS-UMR8502, Université de Paris-Sud, Orsay 91405, France.*
[3]*Laboratoire de Physique Theorique de la Matière Condenseé, UMR 7600,*
Université de Pierre et Marie Curie, Jussieu, Paris-75005, France.
(Dated:)

We study the decoherence of a qubit weakly coupled to frustrated spinbaths. We focus on spin-baths described by the classical Ising spin glass and the quantum random transverse Ising model which are known to have complex thermodynamic phase diagrams as a function of an external magnetic field and temperature. Using a combination of numerical and analytical methods, we show that for baths initally in thermal equilibrium, the resulting decoherence is highly sensitive to the nature of the coupling to the environment and is qualitatively different in different parts of the phase diagram. We find an unexpected strong non-Markovian decay of the coherence when the random transverse Ising model bath is prepared in an initial state characterized by a finite temperature paramagnet. This is contrary to the usual case of exponential decay (Markovian) expected for spin baths in finite temperature paramagnetic phases, thereby illustrating the importance of the underlying non-trivial dynamics of interacting quantum spinbaths.

I. INTRODUCTION

The understanding and control of the decoherence of small quantum systems is central to a lot of recent developments in the fields of nanotechnology and quantum computers[1–5]. For example, the efficacy of qubits, the basic building block of a quantum computer, which can be spin qubits, Josephson junction qubits, charge or flux qubits depends largely on the environments, or baths, to which they are often weakly coupled. The effect of environments on the coherence of the qubit has been studied in various contexts with particular emphasis on bosonic baths[6,7]. In the past few years, the realization of solid state qubits in semiconducting heterojunctions has also resulted in the study of spin baths constituted of spins. At very low temperatures, the decoherence engendered by a spin environment is expected to dominate the loss of the coherence arising from a coupling to phononic degrees of freedom.

In the limit of weak coupling between the qubit and the bath, the effect of intrabath interactions have been explored earlier in other works[8–14]. In some cases, interactions were found to decrease the rate of decoherence, though the exact opposite was seen in cases where the spin bath was on the verge of a standard magnetic quantum phase transition[12]. On the other hand, the qualitative nature of the decoherence i.e., whether it is Markovian or non-Markovian depends largely on the nature of the initial state of the bath[14–17]. For baths at zero temperature, the decoherence is often non-Markovian. Examples include the well known spin-boson model[6], and models of interacting spin environments that we already mentioned above[11,12]. It has also been found in the case of a qubit interacting via the Fermi contact hyperfine coupling with a bath of polarized nuclear spins[15]. How-ever, for baths in thermal equilibrium i.e., at *finite temperatures*, the decoherence in the weak coupling limit is expected to be Markovian as in the case of the spin-boson model. This aspect was also seen in the case of interacting spin baths at finite temperatures[8,10–13]. The associated Markovian decay rate was also found to increase with temperature and, unlike the case of bosons, was found to saturate at high enough temperatures.

Since interactions between spins in condensed matter systems are known to generate a whole range of complex thermodynamic behaviours, it is interesting to ask whether interactions between the bath spins generate novel behaviour for the coherence of a qubit coupled to such a bath. In this general context, various questions arise naturally: does the decoherence contain clear signals about the underlying thermodynamic phase of the bath? Is Markovian decay to be expected for all interacting spin environments at *finite temperatures*, where the bath is in a statistical mixture at temperature T, and not in a pure state[11,18,19]? And can decoherence or others physical quantities asociated with the qubit be used as a sensitive probe of the dynamics of the underlying spin environment?

Here, we shall explore some of these issues by considering the problem of the decoherence of a qubit induced by weak coupling to a model spin-bath with non-trivial dynamics arising from strong frustration and prepared in an initial state which is in thermal equilibrium. Highly frustrated or disordered baths were partially explored in [10,11] where complete predictions for the decoherence could be made only for the case of a one dimensional Ising bath or for spin shards in the infinite temperature limit. Though these works illustrate the potential richness of interacting environments they also highlight the difficulty and limitations of using analytical methods

to study these problems. We adopt a disordered spin bath described by the meanfield random Ising model in a transverse magnetic field. This environment is characterized by a rich thermodynamic phase diagram which shows a spin-glass to paramagnetic transition as a function of temperature and external magnetic field[20]. The total Hamiltonian for the system is given by

$$H = H_B + H_{SB}$$
$$H_B = \sum_{i<j}^{N} J_{ij}\sigma_i^x \sigma_j^x + h\sum_{i=1}^{N} \sigma_i^z$$
$$H_{SB} = \sigma_c^a \sum_i^{N} \lambda_i \sigma_i^a \qquad (1)$$

where H_B is the bath hamiltonian and H_{SB} denotes the spin-bath interaction. The Pauli matrices $\boldsymbol{\sigma}_c$ and $\boldsymbol{\sigma}_i$ denote the spin of the qubit and the i-th spin of the bath respectively. The exchange energies J_{ij} are quenched random variables with a probability distribution $P(J) = \frac{1}{\sqrt{2\pi}\Delta}e^{-J^2/2\Delta^2}$, where the standard deviation of the distribution Δ sets the unit of energy. The qubit couples to the bath operator $V^a = \sum_i^N \lambda_i \sigma_i^a$, with a representing either the z or the x component of the spins. The coupling constants λ are also taken to be quenched random variables. The physics of the bath is described by H_B, the random transverse Ising model (RTIM) which is known to have the following phase diagram: at zero temperature, for transverse fields smaller than a critical field h_c, i.e., $h < h_c$, the system is in a spin glass phase[21]. For $h > h_c$ the system is magnetized with a gap in its spectrum. At finite temperatures, the spin glass order survives up to a critical temperature $T_{sg}(h)$[22,23]. A physical system which is expected to be reasonably described by the above model is LiHo$_x$Y$_{1-x}$F$_4$, where the Ho concentration, x, tunes the system between different physical regimes[24]. It has been proposed as a minimal toy model to investigate the effects of quantum entanglement of spins[25]. The critical temperature T_{sg}, that sets the value of the coefficient Δ, is of the order of 1K[24], in the compounds. Consequently, the effective high temperature paramagnetic phases we study in this paper correspond to rather low real temperatures, where we expect the spin environment to dominate and phononic contributions to the decoherence can be neglected. There have also been propositions for engineering model magnetic environments with very small energy scales using cold atoms[13].

We note that in the spin glass phase, only the correlations involving the x-component of the spin exhibit spin glass features whereas the correlation of the S_z components merely exhibit a gap. Clearly, it would be interesting to explore the effect of these phases on the decoherence of the qubit. Moreover, due to the inherent anisotropy of the bath, we expect the decoherence to be dependent on whether the qubit couples to the x or z components of the bath spins. In this paper, we address these questions in the limit of weak qubit-spinbath coupling. Since this problem cannot be studied analytically, we use numerical exact diagonalization methods to calculate the bath eigenstates and eigenvalues and consequently, the resulting decoherence. We obtain a rich spectrum of results for the coherence of the qubit and in particular, a non-Markovian i.e., a non-exponential decay of the coherence at finite temperatures.

The paper is organized as follows: in Sec. II, we present the weak coupling formalism used to calculate the decoherence of the qubit. We present our numerical method in Sec. III and use it to study the analytically tractable case of decoherence induced by an Ising chain spin-bath so as to benchmark our method. We compare our results for the Markovian decoherence rate with known analytical results for an infinitely long chain, so to establish the importance of the finite size effects introduced by our numerical method. In Sec. IV A, we present our results for the decoherence in the weak coupling regime for the long range Sherrington-Kirkpatrick model which has an Ising spin glass phase at low enough temperatures and present a comparison of our results with some analytical results which are known in the high temperature paramagnetic phase. In Sec. IV B, we present in detail our main results for the decoherence induced by the RTIM spin-bath for two different couplings of the qubit to the bath. We conclude with a discussion of our results in Sec. V.

II. WEAK COUPLING FORMALISM

In this section, we summarize the weak coupling formalism[11] used to calculate the decoherence. This approach is valid provided the energy associated with the qubit-bath coupling is smaller than all the scales of the bath. We first assume that at time $t = 0$, the combined system of the central spin and the bath have a factorizable initial density matrix: $\Omega = \rho(0) \otimes \rho_B$. Depending on the coupling of the central spin to the bath operator V^a, the qubit is in a pure state whose basis vectors are defined by $|\psi^a\rangle = \alpha|\leftarrow^a\rangle + \beta|\rightarrow^a\rangle$ $(\rho(0) = |\psi^a\rangle\langle\psi^a|)$ where $|\leftarrow^x\rangle = |\leftarrow\rangle$, $|\rightarrow^x\rangle = |\rightarrow\rangle$ and $|\leftarrow^z\rangle = |\uparrow\rangle$, $|\rightarrow^z\rangle = |\downarrow\rangle$. The bath is chosen to be at thermal equilibrium with temperature $T \equiv 1/\beta$ leading to a density matrix

$$\rho_B = \frac{e^{-\beta H_B}}{Z} \qquad (2)$$

where $Z = \text{Tr}\exp(-\beta H_B)$ is the bath partition function. The time evolved reduced density matrix is given by

$$\rho(t) = |\alpha|^2 |\leftarrow^a\rangle\langle\leftarrow^a| + |\beta|^2|\rightarrow^a\rangle\langle\rightarrow^a| + M(t)\alpha^*\beta|\rightarrow^a\rangle\langle\leftarrow^a| + M(t)^*\alpha\beta^*|\leftarrow^a\rangle\langle\rightarrow^a| \tag{3}$$

where the factor

$$M(t) = \mathrm{Tr}\left(e^{-i(H_B+V^a)t}\,\rho_B\,e^{i(H_B-V^a)t}\right) \tag{4}$$

is a measure of the decoherence induced by the bath at time t[7,11]. Note that Tr denotes the usual trace as H_B and V^a are operators in the bath Hilbert space. For weak coupling to the environment i.e., for small λ, we can use the super-operator formalism[7] to obtain the following form for the decoherence[11], being the Laplace transform of $M(t)$

$$\tilde{M}(z) = -i\int_0^\infty dt\,e^{izt}M(t) \tag{5}$$

where z is a complex variable with Im$z > 0$. As shown in [11], this Laplace transform can be written as

$$\tilde{M}(z) = [z - \Sigma(z)]^{-1} \tag{6}$$

where the self-energy Σ up to second order is given by

$$\Sigma_2(z) = 2\mathrm{Tr}(V^a\rho_B) - $$
$$2i\int_0^\infty dt\,e^{izt}\left[\langle V^a(t)V^a\rangle_c + \langle V^aV^a(t)\rangle_c\right] \tag{7}$$

where the connected correlation functions are defined as

$$\langle V^a(t)V^a\rangle_c = \langle V^aV^a(t)\rangle - \langle V^a(t)\rangle\langle V^a\rangle \tag{8}$$

The coherence M can thus be written in terms of the real functions Λ_2 and Γ_2 defined by

$$\Lambda_2(E) - i\Gamma_2(E) = \lim_{\eta\to 0^+}\Sigma_2(E+i\eta) \tag{9}$$

where E is real. This then leads to the weak coupling result

$$\Theta(t)M(t) = \frac{i}{2\pi}\int dE\frac{e^{-itE}}{E - \Lambda_2(E) + i\Gamma_2(E)} \tag{10}$$

where $\Theta(t)$ is the Heaviside step function and Λ_2 and Γ_2 satisfy standard Kramers-Kronig relations. In general, $\Gamma_2(E)$ might have analytic as well as non-analytic parts. It is interesting to note that in the weak coupling limit, the decoherence is essentially dictated by $\Gamma_2(E)$ which as can be seen from (7) is proportional to the symmetrized dynamic structure factor of the bath.

Typically for spin baths, we encounter situations where, one can have a net magnetization along a certain spin direction $\langle V^a\rangle = \kappa \neq 0$, and/or magnetic ordering where $\langle V^a(t)V^a\rangle_c = \mu + f(t)$ with κ and μ being

constants independent of time, and $f(t)$ a time-varying function. The resulting self energy in the Laplacian variables then takes the form

$$\Sigma_2(z) = 2\kappa + 4\frac{\mu}{z} + g(z) \tag{11}$$

where $g(z)$ is some analytic function of z. For the asymptotic decoherence, the first two terms generate oscillations resulting in a decoherence of the form

$$M(t) = \exp\left(2i\kappa t\right)\cos\left(2\sqrt{\mu}t\right)\tilde{M}(t) \tag{12}$$

where[11]

$$\ln\tilde{M}(t) \simeq -\frac{2}{\pi}\int dE\frac{\sin(tE/2)^2}{E^2}\Gamma_2(E)\quad. \tag{13}$$

and

$$\Gamma_2(E) = [\tilde{f}(E) + \tilde{f}(-E)] \tag{14}$$

being $\tilde{f}$ the Fourier transform of the function $f(t)$. (13) is also known as the time-convolutionless projection operator (TCL) approximation[26]. The true intermediate time decoherence is expected to be lightly modified with respect to the result predicted by (13), but it is expected to be qualitatively similar to that predicted by (10), which is valid for all t. In the absence of any intrinsic dynamics of the central spin, the second order aproximation used here, leads to an equation for the decoherence which resembles that obtained for the spin-boson model[27]. Though (10) is exact for the spin-boson case, here it is valid only in the limit of weak qubit-spinbath coupling. Morevoer, not all spectral densities $\Gamma_2(E)$ obtained from interacting systems can be simulated by the usual non-interacting boson baths.

For the disordered systems studied here, the correlation functions (8) and (7) need to be averaged over the probability distributions of both the exchange interactions J_{ij} and the coupling constants λ_i. In the rest of the paper, the coupling constants λ_i in (1) are chosen to have the following disorder averages: $\overline{\lambda_i} = 0$ and $\overline{\lambda_i\lambda_j} = (\lambda^2/N)\delta_{ij}$ where N is the total number of spins in the bath. This choice leads to the vanishing of the first order correction to the self energy since the disorder average of κ is zero. The disorder averaged Γ_2, is then directly related to the connected local spin correlation functions $\overline{\langle V^aV^a\rangle_c}$, and it is evaluated using the spectral representation for the dynamical structure factor

$$S^{aa}(E) = \int_{-\infty}^{\infty} dt \exp{(iEt)}\overline{\langle V^a(t)V^a \rangle_c}$$

$$= \frac{2\pi\lambda^2}{NM} \sum_{m=1}^{M} \frac{1}{Z^{(m)}} \sum_{i=1}^{N} \sum_{j,k=1}^{2^N} \exp{(-\beta E_j^{(m)})} |\langle j^{(m)}|S_i^a|k^{(m)}\rangle|^2 \times \delta(\omega - E_j^{(m)} + E_k^{(m)}) - 2\pi\lambda^2 m_a^2 \delta(E)$$

$$= 2\pi\mu\delta(E) + \tilde{f}(E) \tag{15}$$

where M is the number of realizations of disorder for the exchange interactions J_{ij} and m_a^2 is the disordered average of the square of the local magnetic moment. Our method for evaluating (15) is presented below.

III. NUMERICAL METHOD

To compute Γ_2 for the RTIM spin-bath we use exact diagonalization methods. The advantage of the full diagonalization is that it permits us to calculate finite temperature quantities as well. We first study the coherence of the qubit coupled to a random Ising chain bath described H_B with the external field set to $h = 0$, where known analytical results can be used to benchmark the implemented numerical method. The interactions in the bath are confined to nearest neighbors on the chain and the spin-bath coupling is taken to be in the $a = z$ direction.

We consider baths with the number of spins N varying from 3 to 10 spins. For a given set of exchange interactions, the resulting hamiltonian which is a $2^N \times 2^N$ matrix is exactly diagonalized and the eigenenergies and functions are obtained. These are then used to compute the dynamical structure factor and $\Gamma_2(E)$. Since the interactions are quenched random variables, we repeat the above procedure for several thousands of realization of disorder and we obtain the disorder averaged Γ_2. In Fig. 1, we plot $\Gamma_2(E)$ for the case of the Ising bath for different sizes of the bath, and fixed temperature $T = 0.01\Delta$. The analytical results for the thermodynamic case are also shown in the graph.

Note that as the number of spins N in the chain increases, the numerical results converge to the analytical curve obtained for a thermodynamic bath. At high E, $\Gamma_2(E)$ is almost independent of the size of the bath. This is due to the fact that the typical energy bonds are of order J_{ij} ($\mathcal{O}(\Delta)$) (independent of the size of the bath), which are sufficiently small to produce any modification in the high energy spectrum. At low energies, size effects are most significant, since at finite sizes there are no exact cancellations that lead to the vanishing of $\Gamma_2(E)$ at $E = 0$. Nevertheless, the spectra shows good uniform convergence as N increases. At higher T, when the thermal energy is higher than the typical energy of the bonds, the convergence is even better and $\Gamma_2(E)$ is roughly independent of the size of the bath. In Fig. 2, we plot the
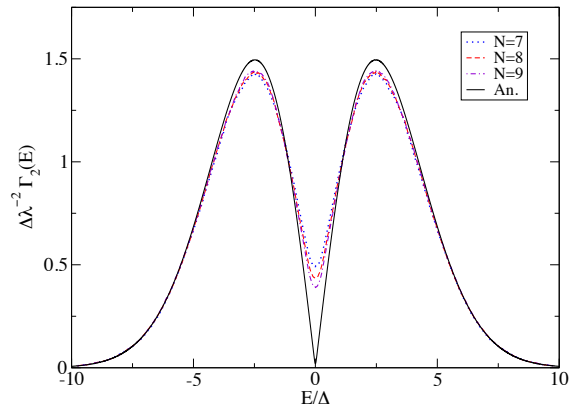

FIG. 1: (Color online) $\Delta\lambda^{-2}\Gamma_2(E)$ as a function of E for $T = 0.01\Delta$ and different N. Note that as N increases, the numerical results approach the analytical result (An.). A similar result is found for the SK long range system.
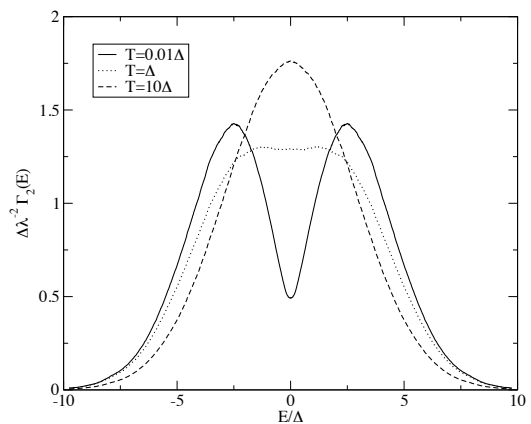

FIG. 2: $\Delta\lambda^{-2}\Gamma_2(E)$ as a function of E for different T for $N = 7$.

variation of $\Gamma_2(E)$ for different temperatures. As shown in Ref. 11, it is the low frequency part that is mainly affected by the temperature effects.

At high T, $\Gamma_2(E)$ is basically a broad peak of width Δ, centered at $E = 0$. This is due to the thermal fluctuations which result in uncorrelated spins, and $\Gamma_2(E)$ merely reflects the distribution of the bonds J_{ij} and the structure of the energy levels. Both temperature and size
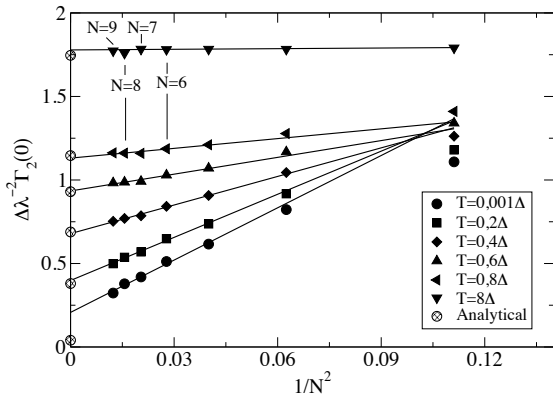
FIG. 3: $\Delta\lambda^{-2}\Gamma_2(0)$ as a function of $1/N^2$. Note the excellent agreement of the extrapolated value of $\Gamma_2(0)$ and the analytical one, except at low T ($T \lesssim 0.2\Delta$).

FIG. 4: $\Delta\lambda^{-2}\Gamma_2(0)$ (extrapolated to the thermodynamic limit) as a function of T. Good agreement with analytical results (dotted curve) except at $T \lesssim 0.2\Delta$ (inset).

effects are seen to have an impact on the low frequency part of $\Gamma_2(E)$ with the consequence that the asymptotic decoherence is more sensitive to thermal fluctuations and finite size effects.

We use our numerical results for $\Gamma_2(E)$ to calculate the decoherence $M(t)$ given by (13). A comparison of our results with the analytical results obtained for the infinite chain[11] permits us to gauge the importance of finite size effects. As for the infinite chain case of Ref. 11, the decoherence for the finite chain can also be analyzed in terms of three regimes described by the two characteristic times: $t_\Delta = \Delta^{-1}$ and $t_\beta = \beta = T^{-1}$. At short times, the coherence is given by the universal gaussian, $\ln M(t) = -t^2(2\pi)^{-1}\int dE\Gamma_2(E)$, given by the sum rule of $\Gamma_2(E)$

$$\int_{-\infty}^{\infty} dE \ \Gamma_2(E) = 4\pi\lambda^2/\Delta \qquad (16)$$

The asymptotic Markovian regime, where the coherence decays exponentially is characterized by the values of $\Gamma_2(E)$ at $E = 0$ (for $t \to \infty$, $\ln M(t) \propto -\Gamma_2(0)t$). At high T, $M(t)$ remains practically constant up to $t \simeq t_\Delta$, where a final Markovian regime arises. When $T \lesssim \Delta$, the gaussian regime is followed by an intermediate time regime where the coherence decay as a power law, before reaching the Markovian regime. A careful inspection of our numerical data shows that, $\Gamma_2(0)$ scales as $1/N^2$ (Fig. 3). The extrapolated values of $\Gamma_2(0)$ for $N \to \infty$ as a function of T are plotted in Fig. 4, where it can be seen that there is an excellent agreement between the analytical values given by[11] $\Gamma_2(0) = 2\pi\lambda^2\int dJ P(J)^2(1 - \tanh(\beta J)^2)$, and the extrapolated values except for $T \lesssim 0.2\Delta$ (inset of Fig. 4). At very small T, since both size effects and temperature effects are non negligible at low energies, we surmise that the accessible system sizes are not sufficient to reach the scaling regime.

To summarize, we see that our numerical method does reproduce the expected analytical behavior for the spin
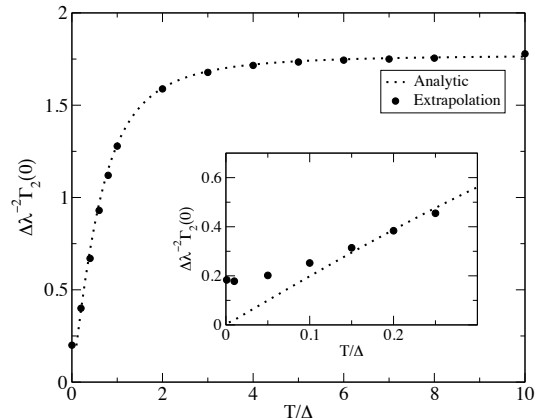
chain bath except at low temperatures where, the Markovian rate is overestimated in our approach. Nonetheless, our results reproduce the existence of the different regimes. We would like to draw attention to the fact that the benchmark case of the chain is in a sense a worst case scenario. In fact, for a 1-d spin-bath one expects to have stronger finite size effects compared to the models to be studied in the rest of the paper: i.e., infinite-range models which are known to have much reduced finite size effects[22,28].

Before leaving this numerical method section we would like to note that our method differs substantially from others that are based on the solution of finite size clusters and cluster expansions. Those methods usually deal with a non-disordered model hamiltonian, which is solved for a small system size. The finite size effects are dealt with by implementing various cluster expansion schemes. In those cases, the finite nature of the cluster provides a discrete pole structure with a finite low energy cut-off and hence a finite recursion time that provides a long time cut-off for the study of the decoherence effects. In our case the situation is different. The effect of the bath enters through the spin susceptibility, and this quantity in a disordered model is computed through the disorder average. Since we have a continuous (Gaussian) distribution of couplings, the disorder-averaged susceptibility, though computed on finite size clusters, does not have a finite low-energy cut-off. Therefore, the decoherence does not have a finite recursion time. All the systematic errors in our approach are due to the second order approximation, which is safe so long the coupling between the qubit and the bath is small, and to the finite size of the clusters that are diagonalized to compute the susceptibility of the bath's Hamiltonian. This latter quantity can be, nevertheless, extrapolated to large system sizes, as we shall see latter. This is validated by the benchmark of the method against an analytically solvable case that we describe in the beginning of next section.

6

IV. MODELS OF SPINS BATHS

In this section, we apply our numerical method to study the decoherence induced by interacting quantum spin-baths which do not have conventional magnetic order like ferromagnetism or antiferromagnetism. The models studied all have infinite range interactions: i.e., all spins interact with each other which leads to the presence of a significant geometric frustration. Similar models have been studied in Ref. 10, where the focus was on the nature of the distribution of the energy level spacings and their impact on the decoherence. A standard lore is that thermal fluctuations in the weak coupling regime always leads to a Markovian i.e., exponential decoherence. Here, we will discuss cases, where the decoherence remains highly non-Markovian in certain finite temperature paramagnets.

A. Infinite-ranged Ising bath with $h = 0$

We study the decoherence induced by the infinite-range random Ising bath also known as the Sherrington-Kirkpatrick (SK) model[29]. For a gaussian distribution with zero mean of the exchange interactions between the spins, the system is paramagnetic except below the spin-glass transition temperature $T \leq T_{sg} = \Delta$ where the system develops spin glass order. Note that for the infinite range model, extensiveness of the free energy requires as to scale the interactions $J_{ij} \to J_{ij}/N$. In this case, there is no first order contribution to the self energy and the second order contribution is given directly by the full correlation function as opposed to the connected correlation function of (8) i.e., both $\kappa = \mu = 0$. Moreover, Γ_2 is proportional to the probability distribution of the local magnetic fields as discussed in Ref. 11. This distribution is straightforward to evaluate analytically in the paramagnetic phase, but numerical methods are required to obtain the same in the spin glass phase. Earlier work only discussed the evolution of the Markovian rate close to the spin glass transition temperature[11]. Here, we compute the coherence for all times and find an asymptotic Markovian regime at all finite temperatures. Our results are shown in Fig. 5 and we see that they qualitatively resemble the results obtained for the Ising chain. Moreover, our method reproduces known analytical results in the paramagnetic phase and also approaches the expected linear behavior of Γ at low frequencies as $T \to 0$[29].

The numerical results for $\ln M(t)$ are shown in figure 6. At short times, $t \lesssim t_\Delta \equiv 1/\Delta$, the sum rule obeyed by Γ_2 ensures that $M(t)$ decays as a gaussian akin to the free spin bath. For times $t > t_\Delta$, temperature starts playing a relevant role. At high $T > T_{sg}$, since $\Gamma_2(E)$ is a peak of width $\mathcal{O}(\Delta)$ cf. Fig. 5, $M(t)$ decays as a Markovian for all times $t \sim t_\Delta$. For $T \ll T_{sg}$, the asymptotic Markovian regime is preceded by a power law regime resulting from the partial linear behavior of $\Gamma_2(E)$ for small E. As
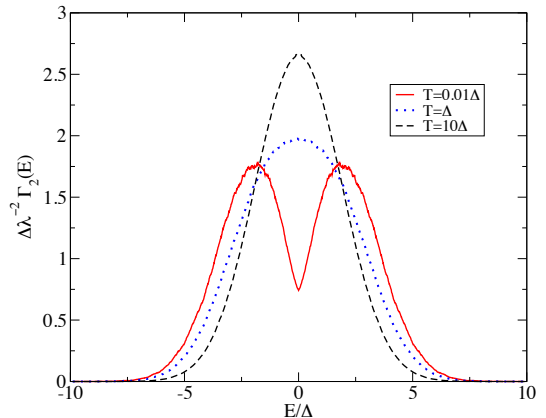

FIG. 5: (Color online) $\Delta\lambda^{-2}\Gamma_2(E)$ for different values of T and $N = 9$, for the SK bath. The results are qualitatively similar to that of the chain.
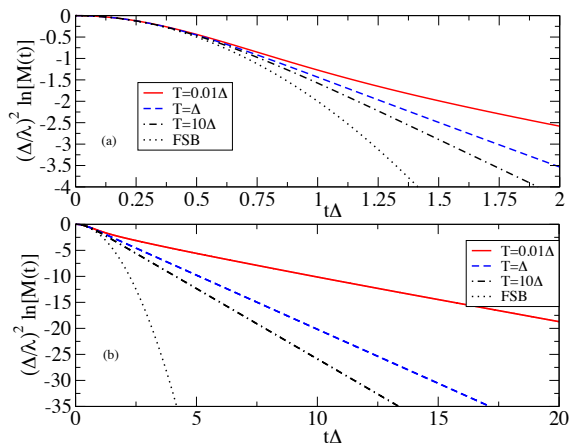

FIG. 6: (Color online) $(\Delta/\lambda)^2 \ln M(t)$ for the SK bath and the comparison with the free spin-bath (FSB); (a) for short times, where it can be seen that at $T = \Delta$, there's a change of the curvature in $\ln M(t)$; (b) for long times.

$T \to 0$, this intermediate power law regime is expected to extend to the asymptotic regime. This is however, hard to infer from the numerics, since finite size effects smear the value of $\Gamma_2(0)$ and hence, the linear behavior of $\Gamma_2(E)$ predicted by the TAP-method calculation [30]. Nevertheless, we see that as T decreases from the paramagnetic phase, $\Gamma_2(0)$ decreases and the linear contribution to $\Gamma_2(E)$ become more significant. Extrapolating the results of $\Gamma_2(0)$ to the limit of $N \to \infty$ to obtain the Markovian decay rate in the thermodynamic limit, we find that $\Gamma_2(0)$ scales $1/N$ cf. Fig. 7 (instead of the $1/N^2$ scaling in the Ising chain). The resulting Markovian rate is plotted as a function of T in Fig. 8, and perfectly matches the analytical values predicted in [11] in the PM-phase. As before, there is a mismatch of the results in the very low temperature regime, probably because our system sizes do not access the scaling regime.
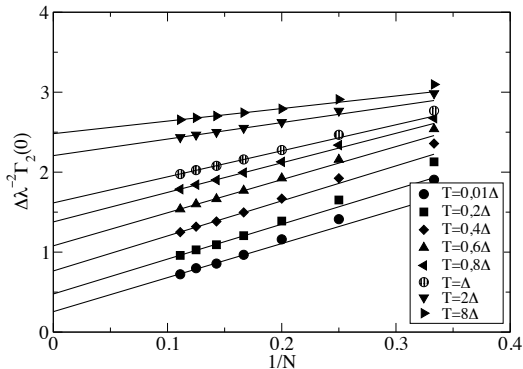
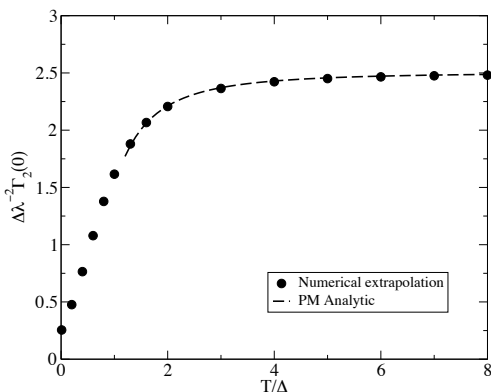FIG. 7: Scaling plot for $\Delta\lambda^{-2}\Gamma_2(0)$ as a function of $1/N$ for the SK bath.

FIG. 8: $\Delta\lambda^{-2}\Gamma_2(0)$ (extrapolated to the thermodynamic limit) as a function of T for the SK bath. The dashed curve represents the analytical results in the paramagnetic phase.

As in the case of the Ising chain, we find that interactions between the spins do lead to longer coherence times as opposed to the case of a free spin bath. The only visible effect of the spin glass phase transition is the point of inflexion in the curvature of $\ln M(t)$ for $t \simeq t_\Delta$ when the asymptotic Markovian regime takes over. This curvature is negative for $T > T_{sg}$ and positive for $T < T_{sg}$. The absence of a radical change in the decoherence is not surprising since the qubit does not couple to the operator which corresponds to the spin glass order parameter.

In the following section, we study the RTIM which is known to have both, a quantum phase transition at $T = 0$, and a finite temperature classical phase transition. We study two different couplings between the qubit and the bath spin operators and show that the nature of these couplings has highly non-trivial consequences for the decoherence.

B. Sherrington-Kirkpatrick model in a transverse field $h \neq 0$

The Sherrington-Kirkpatrick model in a transverse field (RTIM) is a more interesting case than the previously studied $h = 0$ case. At $T = 0$, the system undergoes a phase transition from a spin glass state for $h \leq h_c \simeq 1.44\Delta$ to a gapped phase for $h \geq h_c$. As temperature is increased, the spin glass phase disappears at a finite temperature which depends on the value of the magnetic field. The magnetic field h is therefore, expected to deeply influence the behavior of $\Gamma_2(E)$, and hence the coherence of the central spin. Since the model is not isotropic, it is important to note that the spin glass order exists only along the x component of the spin. To probe the physical ramifications of this anisotropy, we examine two different couplings of the central spin to the bath: a coupling of the spin operators in the direction of the field ($a = z$) and a coupling perpendicular to the field ($a = x$). As we will show below, these lead to radically different predictions for the decoherence. Previous numerical studies[22] of this model have shown finite size effects to be rather minimal. Given the numerical complexities in the vicinity of the phase transition, we limit the scope of the present study to consider two values of the field $h = 0.1h_c$ and $h = 2h_c$, that set the system in qualitatively different regimes.

1. Coupling parallel to the field (case $a = z$)

Since a magnetic moment is present in the z direction for $h \neq 0$, the $\Gamma_2(E)$ is given by the full connected correlation function (8). As shown in (15), this contributes a singular term $\propto \mu\delta(E)$ to $\Gamma_2(E)$ which then leads to oscillations in $M(t)$ (equation 12). An unambiguous way to extract the coefficient μ is via the sum rule satisfied by the dynamical structure factor[22]. This, however, is numerically cumbersome and in the rest of the paper, we do not deal explicitly with these singular terms, since they only induce oscillations and instead concentrate on the non singular part of $\Gamma_2(E)$ that leads to a decay of the coherence. The $T = 0$ behavior of $\Gamma_2(E)$ when a small field $h = 0.1h_c$ is applied is shown in figure 9. We note that even for such small fields, $\Gamma_2(E)$ is radically different from the earlier case of $h = 0$.

Our results for $\Gamma_2(E)$ obtained for $N = 9$ are shown in Figs. 9 and 10, for the small and large field case respectively. In the former, with $h = 0.1h_c$, $\Gamma_2(E)$ exhibits a gap of order $2h$ at $T = 0$ (numerically, the $T = 0$ curve is indistinguishable from the $T = 0.1\Delta$ curve shown in Fig. 9). At high T, $\Gamma_2(E)$ shows a pronounced peak around $E \simeq \pm 0.1h$ and broader peaks of width $\approx 4\Delta$ in the background. Similar features are seen at high magnetic fields (Fig. 10): existence of a gap $2h$ at $T = 0$ and a two peak structure of width 4Δ at high temperatures. For high enough T, the susceptibility at low frequencies becomes linear with a temperature dependent
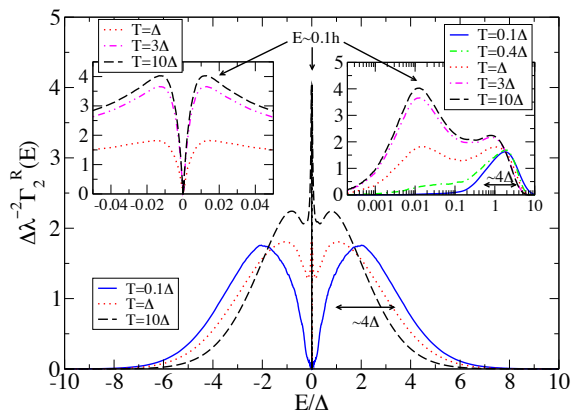
FIG. 9: (Color online) $\Delta\lambda^{-2}\Gamma_2(E)$ for different T, with $N = 9$ and magnetic field set to $h= 0.1h_c$. Note the completely different behavior from the case $h = 0$ (Fig. 5, at small T, $\Gamma_2(E)$ is gapped (right inset, $\Gamma_2(E)$ in a logarithmic scale). For higher T (left inset), $\Gamma_2(E)$ is linear at low energies. We note that the $T = 0$ curve is indistinguishable from the one at $T = 0.1\Delta$.
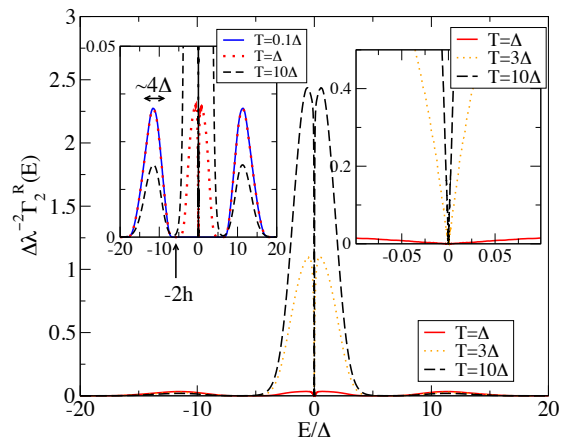

FIG. 10: (Color online) $\Delta\lambda^{-2}\Gamma_2(E)$ for different T, with fixed $N = 9$ and field $h= 2h_c$(the $T = 0$ curve is not plotted here since is indistinguishable from that of $T = 0.1\Delta$). Right inset: behavior for low E. Left inset: high frequency peaks. The missing spectral weight is carried by the $\delta(E)$ term described in the text.

slope, $\Gamma(E) = \alpha(T)|E|$ as $E \to 0$. Note however, that in the high field case the $\delta(E)$ term arising from moment formation carries most of the spectral weight at $T = 0$, as the spectral weight of the regular part of $\Gamma_2(E)$ decreases dramatically. The principal difference between the high and low field case is the presence of the sharp peak around $E \sim 2h$ in the low field case. We have studied the finite size scaling of $\Gamma_2(E)$ and we find that the features mentioned above are robust to finite size effects. Moreover, contrary to the previous cases, here we obtain a good convergence with system size in the low frequency regime.

Interestingly, our results bely the naive expectation that the behavior in the high temperature paramagnetic phase be independent of the values of h considered here. This can be attributed to the fundamental difference between the structure of eigenfunctions and eigenvalues in the two cases: for $h = 0.1h_c$, they correspond to that of a spinglass system, while the high field case essentially correspond to spins in a strong field where the interactions between the spins can be viewed as a perturbation. At high enough temperatures, all eigenfunctions and eigenvalues contribute equally to the $\Gamma_2(E)$ thus the large T regime actually reveals the "geometric" underlying structure of the Hamiltonian, rather than a naively expected universal paramagnetic regime of free spins. This observation remains relevant for all the different spin-models analyzed in this work.

The results for $\Gamma_2(E)$ indicate a very rich evolution of the coherence of the central spin, particularly at long times. We first analyze the results for $M(t)$ plotted in Figs. 11 (high T) and 12 (low T), for $h = 0.1h_c$. As before, for $t \lesssim t_\Delta$, the sum rule obeyed by $\Gamma_2(E)$ (16) dictates an universal gaussian decay for the decoherence, independently of h, Δ and T. This is indeed verified by
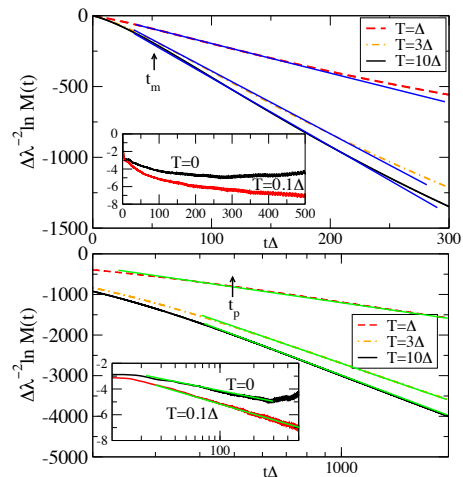

FIG. 11: (Color online) $(\Delta/\lambda)^2 \ln M(t)$ with $h = 0.1h_c$. The upper graph (linear scale), shows an intermediate time Markovian regime ($t > t \simeq t_m$), while the lower graph (logarithmic scale) shows a final power law regime $t > t \simeq t_p$). Insets: $\ln M(t)$ for low T.

our results.

For $T = 0$ (insets of Fig. 11), the decoherence is only partial due to the presence of a gap in $\Gamma_2(E)$ and shows oscillations with a frequency proportional to the size of the gap. Similar oscillations are also seen at very low temperatures. The short time regime $t < t_\Delta$ is followed by a power-law regime for $t > t_p$ which saturates to a finite value at long times. As T increases, the short time and asymptotic power law regime are separated by an intermediate Markovian regime for $t_m < t \ll t_p$. For comparison, the coherence for a bath with $N = 10$ spins
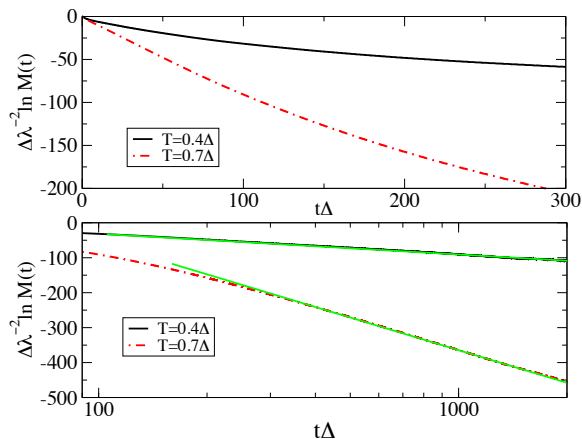
FIG. 12: (Color online) $(\Delta/\lambda)^2 \ln M(t)$ with $h = 0.1h_c$. The upper graph (linear scale), in contrary to the high T coherence of Fig. 11, does not show an intermediate Markovian regime, while the lower graph (logarithmic scale) shows a final power law regime in which t_p increases with T.
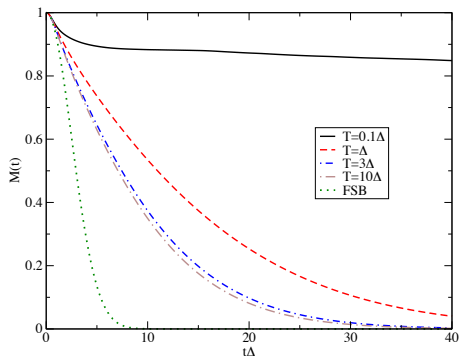

FIG. 13: (Color online) Coherence of the central spin as a function of time, for a bath of $N = 10$ spins for $h = 0.1h_c$ and a bath-qubit coupling $\lambda = 0.2\Delta$. The free spin case (FSB) is also plotted for reference.

is plotted in figure 13 various T. As in the case for $h = 0$, not dramatic change is seen as one traverses the spin glass transition temperature. The existence of an asymptotic power law regime at finite temperatures completely defies the conventional lore that the asymptotic decoherence at finite temperatures is Markovian[18,19]. A systematic analysis of our numerical results indicates that for low fields, t_p is an increasing function of temperature. This implies that in the high temperature paramagnetic phase, the power law regime is pushed to ultra long times and the decoherence is Markovian for realistic times. Though the exact values of t_p and t_m are subject to finite size effects, we have studied various system sizes and find that the intermediate Markovian and power law regimes will survive in the thermodynamic limit.

Before moving on to the high magnetic field case, we shall present an intuitive physical picture of the very low

field case. We first recall the physical picture of the spin-glass ground state at $T = 0$ and $h = 0$, that was discussed in the numerical investigation of Ref. 22. There it was argued that the spin system can be viewed as a coexisting collection of large non-frustrated clusters of spins with few remnant strongly frustrated "dangling" spins. Thus, the dangling spins experience a distribution of effective magnetic fields h_{eff} which, from the work of Sherrington and Kirkpatrick is known to have a linear distribution. This linear is directly reflected in the $\Gamma_2(E) \sim |E|$ that we discussed before.

Now, when a small external magnetic field is turned on, the unfrustrated spins of the clusters will remain essentially unaffected. In contrast, the dangling spins will align in the direction of $\max(h_{\text{eff}}, h)$. This means that the finite external field h will act as a low frequency cut-off, pushing spectral weight towards higher frequencies and thus opening an h-controlled gap in $\Gamma_2(E)$ around $E = 0$ (see the low-T curve of the right inset of Fig. 9). This behavior is in stark contrast with the reference case $h = 0$ presented in section IV A where $\Gamma_2(E)$ remains always gapless (Fig. 5). The dramatic change in the low E regime implies also the qualitative change in the long time behavior of the decoherence that we described in the previous section.

This line of argumentation also allows us to qualitatively understand the origin of the linearity of $\Gamma_2(E)$ at high T. In this limit, from (15) we see that all eigenvalues and eigenfunctions contribute to $\Gamma_2(E)$. On the other hand, when $h = 0$, the data of Fig. 5 shows that $\Gamma_2(E)$ is finite as $E \to 0$, so there are plenty of contributions at arbitrary low frequencies, which originate in pairs of quasi-degenerate eigenstates $|n\rangle$ and $|m\rangle$ with eigenenergies $E_n \approx E_m$, which also have a non-vanishing matrix element $s_{nm}^z = \langle n|\sigma_i^z|m\rangle$. When a small external field ($h \ll h_c$) is turned on we may consider it as a perturbation an perform the following qualitative analysis: The (2x2) block of H in the subspace of n and m will read:

$$H_{nm} = \begin{pmatrix} E_o & h s_{nm}^z \\ h s_{nm}^z & E_o \end{pmatrix}$$

where E_o is the quasi-degenerate energy of the states. The effect of the small h is to lift the degeneracy of the pair of levels resulting in a transfer of spectral weight from $E \approx 0$ to higher frequencies. Extending the analysis to all pairs of quasi-degenerate states contributing to $\Gamma_2(E)$ implies the immediate collapse of the finite value of $\Gamma_2(E = 0)$ to zero when $h \neq 0$, as is seen in our results of Fig. 14. Moreover, the new eigenvalues of H_{nm} are $\approx \pm h s_{nm}^z$, thus with the reasonable assumption of a featureless distribution of the s_{nm}^z matrix elements, we conclude that the degeneracy lifting is uniformly distributed and directly proportional to h. This implies that the behavior of $\Gamma_2(E)$ at very low frequencies should be linear in E with a slope roughly given by $1/h$. This analysis is in qualitative agreement with the low field data shown in Fig. 14.

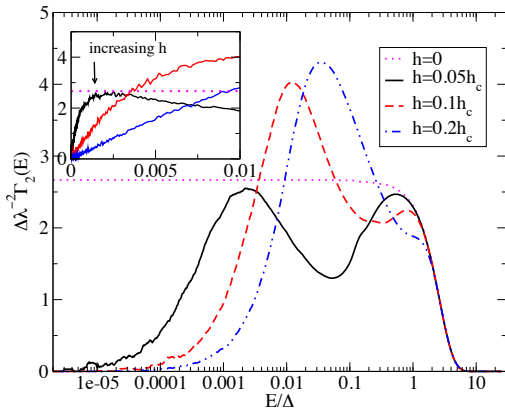At high magnetic fields (Fig. 15), the coherence

FIG. 14: (Color online) $\Delta\lambda^{-2}\Gamma_2(E)$ as a function of E for different values of the field h with $N = 9$ and $T = 10\Delta$. Inset: linear behavior of $\Gamma_2(E)$ for low energies.
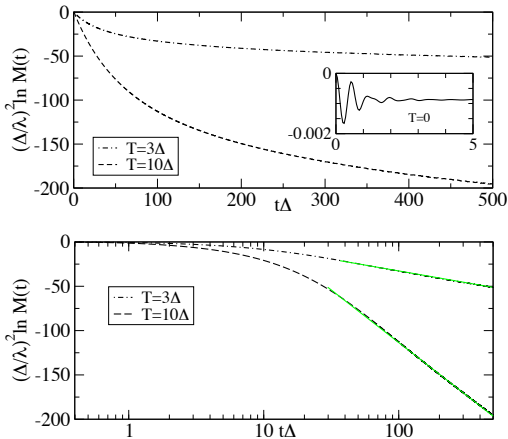

FIG. 15: (Color online) $(\Delta/\lambda)^2 \ln M(t)$ as a function of time for $h= 2h_c$. For low T, since $\Gamma_2(E)$ is gaped, the decoherence is very weak and shows oscillations (inset). As T increases, the coherence decays asymptotically as a power law.

presents a different qualitative behavior. At low T, since $\Gamma_2(E)$ is nearly gapped, and most of the spectral weight is in the $\delta(E)$ term, the central spin decoherence is very weak and shows oscillations. At high T, in contrast to the low h behavior, there is no well defined intermediate Markovian regime, but we recover a power-law decay ($M(t) \propto t^{-\epsilon}$) at asymptotic times. This coefficient ϵ, which characterizes the power law decay, increases with T and saturates to a finite value at very high temperatures, proving that the qubit decoheres faster as temperature increases. The value of the exponent ϵ extrapolated to the thermodynamic limit, as a function of T, is shown in figure 16.
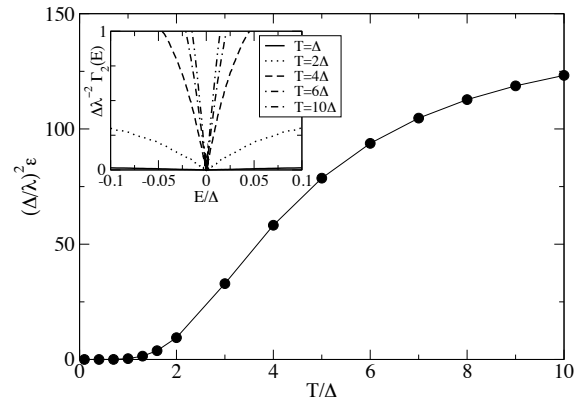

FIG. 16: The exponent ϵ ($M(t) \propto t^{-\epsilon}$) extrapolated to the thermodynamic limit, as a function of T for $h = 2h_c$.

2. Coupling transverse to the field (case $a = x$)

We now explore the case where the qubit couples directly to the bath operator which is related to the spin glass order parameter. In the spin-glass part of the phase diagram ($h \leq h_c$), we now have $\overline{\langle\sigma_x^i\rangle} = 0$ and $\overline{\langle\sigma_x^i\rangle}^2 \neq 0$ $\forall i$. As in Sec. IV B 1, $\Gamma_2(E)$ is again a sum of a regular and a singular contribution. The singular part is a $\delta(E)$ contribution whose strength is related to the spin glass order parameter or Edwards Anderson parameter q_{EA}, $\Gamma_2^{NR} = (4\pi q_{EA} - \sum_i \overline{\langle\sigma_x^i\rangle^2})\delta(E)$. The non-regular part induces oscillations in $M(t)$ and the regular part results in the decay of $M(t)$ (13). The estimation of q_{EA} is a central problem in spin-glasses and as expected our numerics do not produce well converged results of the values of this parameter. q_{EA} is typically estimated by systematically studying $\Gamma_2(E)$ for different sizes of the system, as in Ref. 22. Though it is reasonably straightforward to estimate q_{EA} at $T = 0$, this is not the case at finite temperatures where the delta peak is broadened by both finite size effects and thermal excitations.[22]

When $h = 0$, the operator V^x is constant of motion since $[H_B, V^x] = 0$ resulting in a temperature independent $\Gamma(E) = 4\pi\lambda^2\Delta^{-1}\delta(E)$. As discussed in Sec. II, this results in a purely oscillatory behavior of the form $M(t) = \cos(2\lambda\Delta^{-1}t)$. When the field h is turned on, spin flips are allowed, $[H_B, V^x] \neq 0$ and $\Gamma_2(E)$ has a richer structure. For small h ($h \ll h_c$) and $T = 0$, in addition to a $\delta(E)$ term $\Gamma_2(E)$ has a regular part $\Gamma^R(E) \propto |E|$ as $E \to 0$ and has a peak of width 4Δ, centered around $E = 2h$[22]. As temperature is increased, since q_{EA} is expected to decrease, a part of the spectral weight of the $\delta(E)$ term is transferred to the regular part Γ^R which is now nonlinear at low energies (Fig. 17).

We can now construct a picture of the coherence in the spin-glass phase based on the above description of $\Gamma_2(E)$. The short time behavior is governed by a gaussian. Due to the afore-mentioned problem with the broadening of the delta term, we have not been able to obtain clear pre-
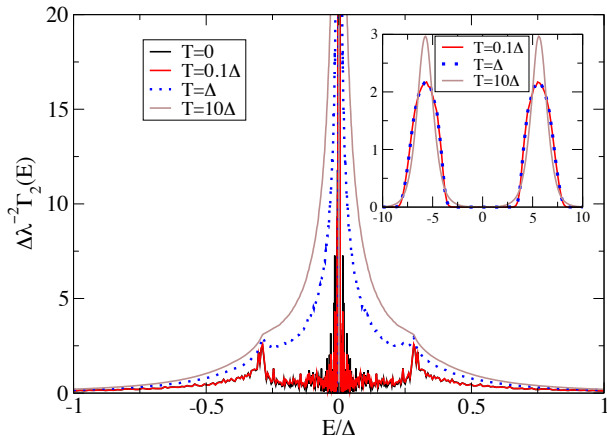
FIG. 17: (Color online) $\Delta\lambda^{-2}\Gamma_2(E)$ for N=9 and field $h=0.1h_c$ for different T. For $T = 0$, $\Gamma_2(E)$ increase linearly for low E and has a maximum at $E = 2h$. As T increases, spectral weight from the $\delta(E)$ (discussed in text) is transferred to low energies. Inset: $\Gamma_2(E)$ for $h = 2h_c$ showing thermal smearing of the gap.
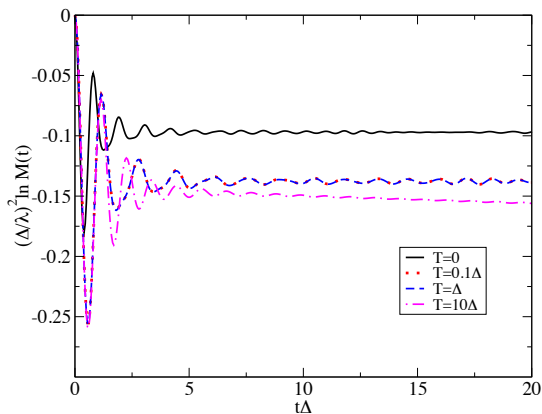

FIG. 18: (Color online) $\Delta\lambda^{-2}\ln M(t)$ for N=9 and field $h=2h_c$ for different T. For $T = 0$, since $\Gamma_2(E)$ is gapped, the decoherence is partial but asymptotic Markovian decoherence is recovered at finite T.

dictions for the intermediate and asymptotic decoherence for low h and low T. This is intimately linked to the underlying spin-glass order since in this case some of the contribution to the singular part exists only in the thermodynamic limit, as opposed to the preceding section, where the singular term arises from a straightforward magnetization of the underlying system and hence one did not have to deal with broadening induced by finite size. Nonetheless, for $T = 0$ and $h \ll h_c$ it is possible

to have a qualitative picture of the coherence. As in the zero-field case, the linearity of $\Gamma_2(E)$ as $E \to 0$ leads to a power-law asymptotic decay of the coherence. At finite temperatures, we expect the asymptotic decay to be Markovian.

For high h ($h > h_c$), there is no spin glass order and hence no singular contribution to $\Gamma_2(E)$. At $T = 0$, the function $\Gamma_2(E)$ is gaped, and it is centered in $E = \pm 2h_c$, with a width of $\sim 4\Delta$. As T is increased, thermal excitations appear within the gap (Fig. 17). Thus, in the former case the decoherence is partial (Fig. 18) and we see oscillations with a frequency given by the gap size. As T increases, thermal excitations start to fill the gap and $M(t)$ decays in a Markovian way given by the value of $\Gamma_2(0)$. This behavior conforms to the usual expectations of asymptotic Markovian decay at finite temperatures and is very different from the small h case.

V. CONCLUSIONS

In this paper, we have used exact diagonalization methods to study the decoherence of a central spin induced by spinbaths with random interactions. We find that the asymptotic decoherence is intricately linked with the nature of the interactions in the bath. Moreover, for a given set of bath parameters, the decoherence crucially depends on the nature of the coupling between the qubit and the bath spins. For the cases of the random transverse Ising model studied here, we find that the underlying nature of the eigenstates of the bath hamiltonian play a preponderant role in determining the decoherence even in the finite temperature paramagnetic phase. More precisely, we find that the decoherence in some of the finite temperature paramagnetic phases is strongly non-Markovian. We emphasize that standard Markovian approximations used to obtain the density matrix and the decoherence at finite temperatures should not be used blindly as they can lead to highly misleading results as in the present case of disordered interacting systems. Unfortunately, we have not been able to study the decoherence in the vicinity of the phase transitions in the bath (both at zero and finite temperatures). This requires the use of other numerical and analytical methods which is beyond the scope of the present work. It will be interesting to study if these features are seen in other highly frustrated spin baths and whether this non-Markovian behavior survives when order corrections to the self-energy are taken into account. These questions are left for future work.

[1] D. Kielpinski, C. Monroe and D. J. Wineland, Nature **417**, 709 (2002).

[2] D. Kielpinski, V. Meyer, M. A. Rowe, C. A. Sackett, W. M. Itano, C. Monroe and D. J. Wineland, Science **291**,

1013 (2001)

[3] B. Trauzettel, D. Bulaev, D. Loss, and G. Burkard, Nat. Phys. **3**, 192 (2007)

[4] J. Fischer and D. Loss, Science **324**, 1277 (2009)

[5] R. Hanson, V. V. Dobrovitski, A. E. Feiguin, O. Gywat and D. D. Awschalom, Science **320**, 352 (2008).

[6] A. O. Caldeira and A. J. Leggett, Phys. Rev. Lett. **46**, 211 (1981); Ann. Phys. **149**, 374 (1983).

[7] U. Weiss, *Quantum dissipative systems* (World Scientific, Singapore, 1993).

[8] S. Paganelli, F. de Pasquale and S.M. Giampaolo, Phys. Rev. A **66**, 052317 (2002).

[9] L. Tessieri and J. Wilkie, J. Phys. A : Math. General. **36**, 12305 (2003).

[10] J. Lages, V. V. Dobrovitski, M. I. Katsnelson, H. A. De Raedt, and B. N. Harmon, Phys. Rev. E **72**, 026225 (2005).

[11] S. Camalet and R. Chitra, Phys. Rev. B **75**, 094434 (2007).

[12] S. Camalet and R. Chitra, Phys. Rev. Lett. **99**, 267202 (2007).

[13] D. Rossini, T. Calarco, V. Giovannetti, S. Montangero and R. Fazio, Phys. Rev. A **75**, 032333 (2007).

[14] J. Fischer and H.-P. Breuer, Phys. Rev. A **76**, 052119 (2007).

[15] W. A. Coish and D. Loss, Phys. Rev. B **70**, 195340 (2004).

[16] W. A. Coish, J. Fischer and D. Loss, Phys. Rev. B **77**, 125329 (2008).

[17] C. Deng and X. Hu, Phys. Rev. B **78**, 245301 (2008).

[18] A. K. Pattanayak and P. Brumer, Phys. Rev. Lett. **79**, 4131 (1997).

[19] M. Lucamarini, S. Paganelli and Stefano Mancini, Phys. Rev. A **69**, 062308 (2004).

[20] K. H. Fischer and J. A. Hertz, Spin Glasses, Cambridge University Press, Cambridge, England (1991).

[21] M. J. Rozenberg and D. R. Grempel, Phys. Rev. Lett. **81**, 2550 (1998)

[22] L. Arrachea and M. J. Rozenberg, Phys. Rev. Lett. **86**, 5172 (2001).

[23] R. Blinc, J. Dolinsek, A. Gregorovic , B. Zalar, C. Filipic , Z. Kutnjak, A. Levstik, and R. Pirc, Phys. Rev. Lett. **83**, 424 (1999).

[24] J. Brooke, D. Bitko, T. F. Rosenbaum and G. Aeppli, Science **284**, 779 (1999)

[25] S. Ghosh, T. F. Rosenbaum, G. Aeppli, and S. N. Coopersmith, Nature **425**, 48 (2003).

[26] A. Royer, Phys. Rev. A **6**, 1741 (1972).

[27] F. K. Wilhelm, M. J. Storcz, U. Hartmann and M. R. Geller, cond-mat/0603637.

[28] L. Arrachea and M. J. Rozenberg, Phys. Rev. B **65**, 224430 (2002).

[29] S. Kirkpatrick and D. Sherrington, Phys. Rev B. **17**, 4384 (1978).

[30] R. G. Palmer and C. M. Pond, J. Phys. F **9**, 1451 (1979).